ChemComm

Accepted Manuscript

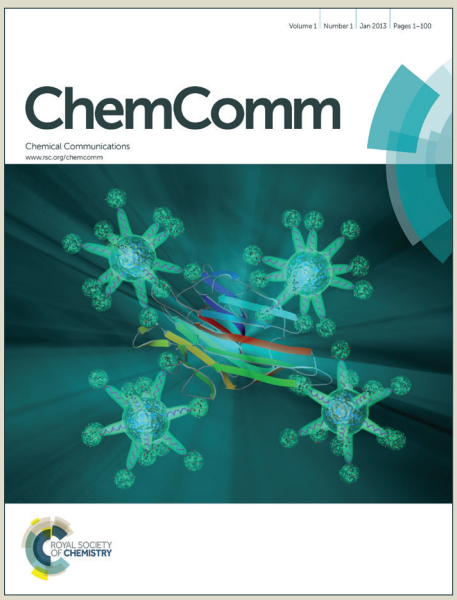

ROYAL SOCIETY OF CHEMISTRY

www.rsc.org/chemcomm

Journal Name

COMMUNICATION

Gathering nanorings via Fe^{2+}-bipyridine coordination

Qingqing Miao,[a] Chunying Yin,[b] Maolin Xie,[c] Yufeng Luo,[a] Zijuan Hai,[a] Qingpan Yuan,[a] Jun Jiang,[c] and Gaolin Liang[a,*]

Received 00th January 20xx,
Accepted 00th January 20xx

DOI: 10.1039/x0xx00000x

www.rsc.org/

Spontaneously precise organization of small structures into complex superstructures is ubiquitous and important in nature. But using small building blocks to mimic this process remains challenge to scientists. Herein, we report the rational design of a bipyridine-derivative 1 and applied it for the self-assembly of nanorings. Addition of Fe^{2+} to the nanorings resulted in the assembly of the nanorings into supernanostructures via Fe^{2+}-bipyridine coordination. HPLC, HR-ESI/MS, UV-vis, DLS, and TEM analyses clearly validated the intramolecular cyclization, self-assembly of nanorings, and additional self-assembly of superstructures via Fe^{2+}-bipyridine coordination. We envision that our strategy to be a new approach of precisely assembling nanostructures of ring shape into more complex superstructures.

It is ubiquitous in nature and in chemistry that small (or small molecular) building blocks are spontaneously organized into complex superstructures via synergistic action of various non-covalent interactions.[1, 2] For examples, proteins,[3] DNA-core-shell nanostructures,[4] and several self-assembling systems such as amphiphilic triblock copolymers,[5] polyelectrolyte,[6] amphiphilic dumbbell-shaped small molecules,[7] organometallic[8] or dendron[9] complexes, and hydrogen-bonded supramolecular disks,[10] have shown their ability of spontaneous organization of ring-shaped superstructures. The precision, elegance, complexity, and functionality of these superstructures pose significant challenge to scientists. Nevertheless, using synthetic molecular building blocks to exploit such smart self-organization processes remains an important step toward the mimicking and understanding of artificial biological systems.[11-14]

Metal-ligand interactions play an important role in natural biological systems. Over the past decade, coordination-based self-assembly system has evolved into a well-established strategy for constructing novel nanostructures via metal-ligand interactions. Among the metal-ligand interactions, metal-bipyridine coordinations are always employed to assemble building blocks into higher order nanostructures. For examples, they are utilized to trigger branched peptide into fiber,[15] promote hollow spheres into self-assembled disks,[16] assemble separated macroscopic gels,[17] self-assemble metallohydrogels.[18] However, to the best of our knowledge, using metal-bipyridine coordination interactions to assemble nanorings into superstructures has not been reported yet.

Inspired by these pioneering studies mentioned above, we aimed to design a metal-promoted self-assembly system to assemble nanorings into superstructures. Our previous studies have shown that **CBT-Cys(SEt)** could self-assemble into nanorings upon reduction-controlled condensation,[19] and bipyridine hydrogel could be used to effectively absorb metal ions.[20] As illustrated in Fig. , we rationally designed a bipyridine-derivative **1** which contains two 2-cyano-6-aminobenzothiazole (CBT) motifs (in blue) and later cysteine groups (in red) for intramolecular macro-cyclization to self-assemble nanorings. A bipyridine motif (in yellow) which links to the side chains of lysine motifs within **1** was designed for the coordination with metal ions after the formation of the nanorings. In detail, upon tris(2-carboxyethyl)phosphane (TCEP)-reduction, the disulfide bonds of **1** were cleaved, initiating the intramolecular condensation reaction to yield macrocyclized product **3**, as demonstrated previously.[21] Then the amphiphilic **3** instantly self-assembled into nanostructures (herein, nanorings) with abundant bipyridine groups on their surfaces. Upon addition of metal ions (herein, Fe^{2+}), the nanorings were gathered together to form higher order nanostructures via Fe^{2+}-bipyridine coordination.

We began the study with syntheses of the precursors and **1** (see in the Supporting Information). The syntheses are facile and straightforward. Briefly, precursor bipyridine-$(Fmoc\text{-}Lys)_2$ (**A**) was synthesized by coupling Fmoc-Lys-OH with 4,4′-dicarboxysuccinimidyl-2,2′-bipyridine and purified with high performance liquid chromatography (HPLC). Then **A** was coupled with Boc-Cys(SEt)-OH to yield **B** using solid phase peptide synthesis (SPPS). By the activation of isobutyl chloroformate (IBCF), **B** was coupled with CBT to yield **C** after HPLC purification. Deprotection of

[a] CAS Key Laboratory of Soft Matter Chemistry, Department of Chemistry, University of Science and Technology of China, 96 Jinzhai Road, Hefei, Anhui 230026, China. E-mail: gliang@ustc.edu.cn (G.-L. L.).
[b] Center for Integrative Imaging, Hefei National Laboratory for Physical Sciences at the Microscale, University of Science and Technology of China, Hefei, Anhui 230026, China
[c] Department of Chemical Physics, University of Science and Technology of China, 96 Jinzhai Road, Hefei, Anhui 230026, China.

† Electronic Supplementary Information (ESI) available: Synthetic routes for precursors and **1**; Fig. S1-S15, Table S1. See DOI: 10.1039/x0xx00000x

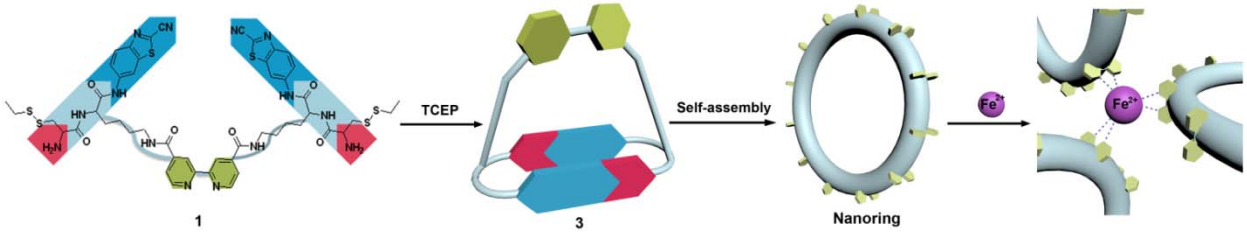

Fig. 1 Schematic illustration of reduction-triggered intramolecular condensation of **1** to yield macro-cyclized product **3**, which instantly self-assembles into nanoring. Upon Fe^{2+} addition, the nanorings were gathered to form supernanostructures via Fe^{2+}-bipyridine coordination.

C yields **1** after HPLC purification.

We then validated the reduction-controlled intramolecular macrocyclization and subsequent self-assembly of nanostructures. After 1.5 h incubation of 100 μM **1** with 4 equiv. of TCEP at room temperature, we directly injected the incubation mixture into a HPLC system and collected the peaks for electrospray ionization mass (ESI-MS) spectroscopic analysis. As shown in Fig. 2, peak on HPLC trace at retention time of 22.4 min (57.4%) was identified as the title product **3** with two intramolecular cyclized structures (Fig. 2b), while that at 21.3 min (39.3%) was identified as the intermediate of **3** (i.e., **2**) only containing one intramolecular cyclized structure (Fig. S6 in the ESI†). Time-course HPLC, in combination of ESI/MS analysis, clearly showed the processes of TCEP-reduction of **1** to yield the reduction product of **1** (i.e., **1-R**) at pH 2, decrease of intermediate **2** and increase of title product **3** with the increase of time at pH 5.5 (Fig. S7 in the ESI†). The theoretically optimized molecular structure of **3**, showing the π-π stacking of the two benzothiazole structures, was displayed in Fig. S8.

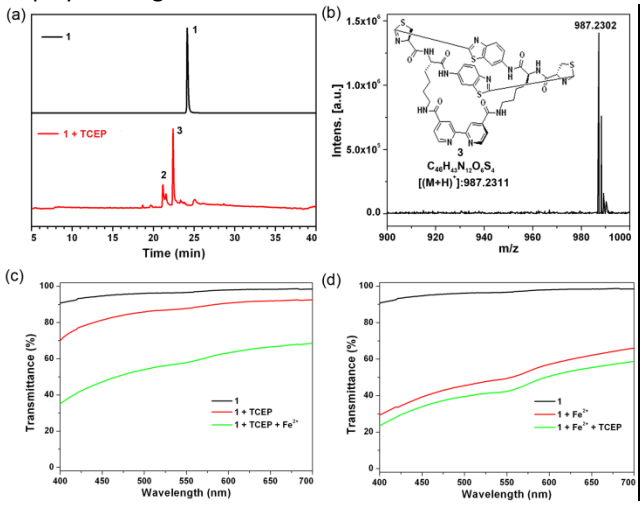

Fig. 2 (a) HPLC traces of **1** (black), 100 μM **1** treated with 4 equiv. of TCEP at room temperature and pH 5.5 for 1.5 h (red). (b) High resolution electrospray ionization mass (HR-ESI/MS) spectrum of HPLC peak at retention time of 22.4 min in Fig. a. (c) Optical transmittance of **1** at 100 μM (black), 100 μM **1** treated with 400 μM TCEP at pH 5.5 for 1.5 h (red), 100 μM **1** treated with 400 μM TCEP for 1.5 h and then treated with 1 mM Fe^{2+} at pH 5.5 for 1 h (green). (d) Optical transmittance of **1** at 100 μM (black), 100 μM **1** treated with 1 mM Fe^{2+} at pH 5.5 for 1 h (red), 100 μM **1** treated with 1 mM Fe^{2+} for 1 h and then treated with 400 μM TCEP for 1.5 h at pH 5.5 (green).

UV-vis, fluorescence spectroscopy and dynamic light scattering (DLS) were then used to monitor the TCEP-triggered formation of nanostructures and Fe^{2+}-bipyridine coordination-induced formation of higher order superstructures. As shown in Fig. 2c, upon the addition of TCEP, UV-vis spectrum of **1** at 400–700 nm (red curve, due to the light scattering of nanostructures) showed an obvious decrease of transmittance compared with that of starting clean solution of **1** (black curve), suggesting the formation of nanostructures in the solution. Interestingly, subsequent addition of Fe^{2+} into above dispersion induced another remarkable decrease of transmittance (28% decrease of the transmittance at 600 nm), suggesting that the presence of Fe^{2+} induced additional dramatic aggregation of the nanostructures in the solution (Fig. 2c). Fluorescence spectra of above three solutions (i.e., **1**, **1** with TCEP, **1** with TCEP and Fe^{2+}) also indicated the occurrence of cyclization and Fe^{2+}-bipyridine coordination (Fig. S9a in the ESI†). In detail, after incubation with TCEP, the fluorescence emission maximum of **1** red-shifted from 416 nm to 437 nm, indicating the formation of luciferin structures. Subsequent addition of Fe^{2+} induced very obvious decrease of the fluorescence emission by 6.9 folds, suggesting the formation of Fe^{2+}-bipyridine complex which severely quenched the fluorescence. In comparison, as shown in Fig. 2d, direct addition of Fe^{2+} to the solution of **1** resulted in dramatic decrease of transmittance (41% decrease of the transmittance at 600 nm), suggesting that Fe^{2+}-bipyridine coordination could induce severe aggregation of **1**. The 5.7 folds of fluorescence quenching of **1** after Fe^{2+} addition also echoed this Fe^{2+}-bipyridine coordination-induced aggregation (Fig. S9b in the ESI†). However, subsequent additional of TCEP to the **1**-Fe^{2+} system only resulted in 7% decrease of the transmittance of **1**-Fe^{2+} at 600 nm (Fig. 2d), suggesting the intramolecular cyclization would not induce additional obvious aggregation of the nanostructures. The red-shift of the fluorescence spectra clearly indicated the occurrence of intramolecular cyclization (Fig. S9b in the ESI†). Moreover, we also used dynamic light scattering (DLS) to characterize the formation of nanostructures and

subsequent superstructures of **1**. As shown in Figure S10a, upon addition of TCEP, the solution of **1** displayed a distinct size distribution averaged at 84 nm, indicating that the self-assembly of nanostructures. Subsequent addition of Fe^{2+} into above dispersion showed bigger size distribution (average size of 318 nm), indicating Fe^{2+} facilitates higher-order assembly. In comparison, as shown in Figure S10b, direct addition of Fe^{2+} to the solution of **1** resulted in the formation of larger aggregates. However, subsequent addition of TCEP to the **1**-Fe^{2+} system induced slight additional aggregation, which echoes well with the transmittance observations. Thus, we concluded that Fe^{2+}-bipyridine coordination after the formation of nanostructures (herein nanorings) would induce further assembly of the nanostructures into superstructures but not vice versa.

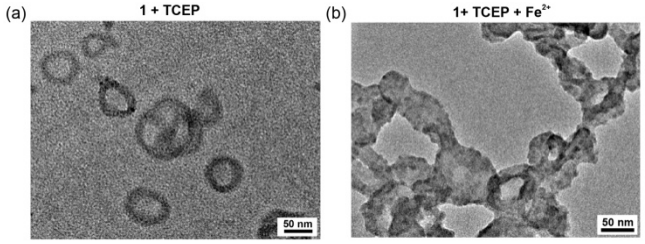

Fig. 3 TEM images of nanorings in the reaction mixture of 100 μM **1** treated with 400 μM TCEP at pH 5.5 for 1.5 h (a), followed by addition of 1 mM Fe^{2+} and then incubated for 1 h (b).

Previous studies have shown that, self-assembly of the condensation products of CBT derivatives resulted in nanostructures of various morphologies including nanofibers,[22] uniform nanoparticles,[23-25] or nanorings.[19] Interestingly, as shown in Fig. 3a and Fig. S11, transmission electron microscope (TEM) images of **1** after TCEP treatment revealed that the condensation product of **1** (i.e., **3**) self-assembled into regular nanorings with an average outer diameter of 56.5 nm and ring width of 12.7 nm. The critical aggregation concentration (CAC) of **1** for the self-assembly of nanorings was measured with the transmittance change at 425 nm of **1** upon TCEP addition at pH 5.5. Plots of the optical transmittance at 425 nm versus the concentration of **1** revealed two regimes, which indicate that the CAC of 31 μM for **1** to form nanorings (Fig. S12a in the ESI†).[26] DLS measurements consistently indicated that the CAC for **1** to self-assemble into nanorings was 31 μM (Fig. S12b in the ESI†).

We then used TEM to investigate the effect of Fe^{2+}-bipyridine coordination on the assembly of as-formed nanorings into higher order nanostructures. Before that, by plotting the absorbance at 565 nm on the UV-vis spectra of **1** before and after Fe^{2+} addition, we confirmed the molar ratio between Fe^{2+} and **1** for the Fe^{2+}-bipyridine coordination to be 1:3 (Fig. S13 in the ESI†). As shown in Fig. 3b, addition of 1 mM $Fe(ClO_4)_2$ (10 times of **1**) to the above nanoring solution resulted in the stacking, condensing, and interconnecting of the nanorings, probably due to the Fe^{2+}-bipyridine coordinations among the nanorings. We also conducted the study of different ratios of Fe^{2+} influencing on the TEM morphologies of the superstructures. As shown in Figure S14a, upon addition of 100 μM $Fe(ClO_4)_2$ (equal molar concentration to **1**) to the nanoring dispersion, several nanorings tend to stick together to form nanoring clusters, suggesting that equivalent Fe^{2+} is enough to assemble nanorings into their clusters but not superstructures. Intrestingly, as shown in Figure S14b, addition of 10 mM $Fe(ClO_4)_2$ (100 times of **1**) to the nanoring dispersion resulted in total interconnection among the nanorings to form superstructures which are similar to those in Figure 3b. As control, TEM image of **1** directly treated with Fe^{2+} only showed amorphous aggregates (Fig. S15a in the ESI†). And addition of TCEP to the **1**-Fe^{2+} dispersion resulted in slight crosslink of the aggregates, as shown by the TEM image in Fig. S15b.

Conclusions

In conclusion, employing a condensation reaction, we rationally designed a bipyridine-derivative **1** and applied it for reduction-controlled self-assembly of nanorings. Follow-up addition of Fe^{2+} to the nanorings resulted in a secondary assembly of the nanorings into supernanostructures via Fe^{2+}-bipyridine coordination. Our strategy provided a new approach of precisely assembling ring-shaped nanostructures into more complex superstructures.

Acknowledgements

This work was supported by Collaborative Innovation Center of Suzhou Nano Science and Technology, the Major Program of Development Foundation of Hefei Center for Physical Science and Technology, and the National Natural Science Foundation of China (Grants 21175122 and 21375121).

Notes and references

1 S. Yagai, S. Mahesh, Y. Kikkawa, K. Unoike, T. Karatsu, A. Kitamura and A. Ajayaghosh, *Angew. Chem. Int. Ed.*, 2008, **47**, 4691.
2 Y. J. Mao, T. Su, Q. Wu, C. A. Liao and Q. G. Wang, *Chem. Commun.*, 2014, **50**, 14429.
3 J. C. T. Carlson, S. S. Jena, M. Flenniken, T. F. Chou, R. A. Siegel and C. R. Wagner, *J. Am. Chem. Soc.*, 2006, **128**, 7630.
4 K. K. Zhang, H. Miao and D. Y. Chen, *J. Am. Chem. Soc.*, 2014, **136**, 15933.
5 D. J. Pochan, Z. Y. Chen, H. G. Cui, K. Hales, K. Qi and K. L Wooley, *Science*, 2004, **306**, 94.
6 H. Flores, J. L. Menchaca, F. Tristan, C. Gergely, E. Perez and F. J. G. Cuisinier, *Macromolecules*, 2005, **38**, 521.
7 J. K. Kim, E. Lee, Z. G. Huang and M. Lee, *J. Am. Chem. Soc.*, 2006, **128**, 14022.
8 W. Lu, S. S. Y. Chui, K. M. Ng and C. M. Che, *Angew. Chem. Int. Ed.*, 2008, **47**, 4568.
9 C. Kaewtong, G. Jiang, M. J. Felipe, B. Pulpoka and R. Advincula, *ACS Nano*, 2008, **2**, 1533.

10 S. Yagai, H. Aonuma, Y. Kikkawa, S. Kubota, T. Karatsu, A. Kitamura, S. Mahesh and A. Ajayaghosh, *Chem. Eur. J.*, 2010, **16**, 8652.
11 A. Ajayaghosh and V. K. Praveen, *Acc. Chem. Res.*, 2007, **40**, 644.
12 G. M. Whitesides and B. Grzybowski, *Science*, 2002, **295**, 2418.
13 J. W. Zhang, C. W. Ou, Y. Shi, L. Wang, M. S. Chen and Z. M. Yang, *Chem. Commun.*, 2014, **50**, 12873.
14 K. Zhu, J. Z. Shen, R. Dietrich, A. Didier, X. Y. Jiang and E. Martlbauer, *Chem. Commun.*, 2014, **50**, 676.
15 D. E. Przybyla and J. Chmielewski, *J. Am. Chem. Soc.*, 2008, **130**, 12610.
16 D. E. Przybyla, C. M. R. Perez, J. Gleaton, V. Nandwana and J. Chmielewski, *J. Am. Chem. Soc.*, 2013, **135**, 3418.
17 Y. Kobayashi, Y. Takashima, A. Hashidzume, H. Yamaguchi and A. Harada, *Sci.Rep.*, 2013, **3**, 1243.
18 Y. Zhang, B. Zhang, Y. Kuang, Y. Gao, J. F. Shi, X. X. Zhang and B. Xu, *J. Am. Chem. Soc.*, 2013, **135**, 5008.
19 Y. Yuan, J. Zhang, M. J. Wang, B. Mei, Y. F. Guan and G. L. Liang, *Anal. Chem.*, 2013, **85**, 1280.
20 Q. Q. Miao, Z. Y. Wu, Z. Hai, C. L. Tao, Q. P. Yuan, Y. D. Gong, Y. F. Guan, J. Jiang and G. L. Liang, *Nanoscale*, 2015, **7**, 2797.
21 D. J. Ye, A. J. Shuhendler, L. N. Cui, L. Tong, S. S. Tee, G. Tikhomirov, D. W. Felsher and J. H. Rao, *Nat. Chem.*, 2014, **6**, 519.
22 S. Liu, A. Tang, M. Xie, Y. Zhao, J. Jiang and G. Liang, *Angew. Chem. Int. Ed.*, 2015, **54**, 3639.
23 Q. Q. Miao, X. Y. Bai, Y. Y. Shen, B. Mei, J. H. Gao, L. Li and G. L. Liang, *Chem. Commun.*, 2012, **48**, 9738.
24 Y. Yuan, H. Sun, S. Ge, M. Wang, H. Zhao, L. Wang, L. An, J. Zhang, H. Zhang, B. Hu, J. Wang and G. Liang, *ACS Nano*, 2015, **9**, 761.
25 D. J. Ye, A. J. Shuhendler, P. Pandit, K. D. Brewer, S. S. Tee, L. N. Cui, G. Tikhomirov, B. Rutt and J. H. Rao, *Chem. Sci.*, 2014, **5**, 3845.
26 X. Z. Yan, S. J. Li, T. R. Cook, X. F. Ji, Y. Yao, J. B. Pollock, Y. H. Shi, G. C. Yu, J. Y. Li, F. H. Huang and P. J. Stang, *J. Am. Chem. Soc.* , 2013, **135**, 14036.